Available online at www.sciencedirect.com
SCIENCE DIRECT®
Surface Science 564 (2004) 156–164
SURFACE SCIENCE
www.elsevier.com/locate/susc

Morphology, structure, and electronic properties of $Ce@C_{82}$ films on Ag:Si(1 1 1)-($\sqrt{3}\times\sqrt{3}$)R30°

L. Wang [a], K. Schulte [a], R.A.J Woolley [a], M. Kanai [b], T.J.S. Dennis [b], J. Purton [c], S. Patel [c], S. Gorovikov [d], V.R. Dhanak [c,e], E.F. Smith [f], B.C.C Cowie [g], P. Moriarty [a,*]

[a] *School of Physics and Astronomy, University of Nottingham, University Park, Nottingham NG7 2RD, United Kingdom*
[b] *Department of Chemistry, Queen Mary University of London, London E1 4NS, United Kingdom*
[c] *Daresbury Laboratory, Daresbury, Warrington, Cheshire WA4 4AD, United Kingdom*
[d] *Max Lab, Lund University, P.O. Box 118, S-221 00 Lund, Sweden*
[e] *Department of Physics, University of Liverpool, Liverpool L69 3BX, United Kingdom*
[f] *Centre for Surface Chemical Analysis, School of Chemistry, University of Nottingham, Nottingham NG7 2RD, United Kingdom*
[g] *European Synchrotron Radiation Facility, B.P. 220, F-38043 Grenoble Cedex, France*

Received 20 March 2004; accepted for publication 24 June 2004
Available online 6 July 2004

Abstract

The adsorption behaviour and electronic properties of $Ce@C_{82}$ molecules on the Ag:Si(1 1 1)-($\sqrt{3}\times\sqrt{3}$)R30° surface have been studied using scanning tunnelling microscopy and photoelectron spectroscopy. Submonolayer coverages and multilayer films of $Ce@C_{82}$ comprise highly ordered molecular domains which have a single, well-defined orientation with respect to the underlying substrate crystallographic axes. UPS spectra reveal that the $Ce@C_{82}$ films are semiconducting with a band gap of at least 0.3 eV and, as for $La@C_{82}$, contain low binding energy peaks related to charge transfer from the encapsulated atom to the fullerene molecular orbitals. The valence state of the incarcerated Ce has been probed by Ce 3d XPS for both 'as-deposited' and air-exposed $Ce@C_{82}$ monolayers. There is little change in the 'close to 3+' valence state of the Ce atom—and little evidence of Ce oxidation—following exposure of a $Ce@C_{82}$ monolayer to atmosphere for a period of 10 months.

Keywords: Fullerenes; Photoemission (total yield); Scanning tunneling microscopy

* Corresponding author. Tel.: +44 0115 9515156; fax: +44 0115 9515180.
E-mail address: philip.moriarty@nottingham.ac.uk (P. Moriarty).

0039-6028/$ - see front matter © 2004 Elsevier B.V. All rights reserved.
doi:10.1016/j.susc.2004.06.189

1. Introduction

Ever since their successful synthesis and purification shortly after the discovery of C_{60} [1,2], endohedral fullerenes [1] have attracted wide attention as a new family of molecules with unique structural and electronic properties. In an endohedral fullerene, one or more atoms are incorporated into the inner cavity of the fullerene cage [3]. The encapsulated atom usually—though not always (see below)—transfers charge, where the amount of charge transfer depends on the type of the encapsulated atom(s), to the carbon cage. This provides a novel method of fullerene doping. A wide variety of experimental studies have conclusively shown that, in the majority of cases, the interaction of the encapsulated atom with the cage generally has a strong ionic component [4] and that a substantial degree of orbital hybridisation may also be present [5]. Despite this coupling, the fullerene shell can provide efficient isolation of the encapsulated atom from the molecular surroundings. The clearest example of this shielding effect is the 'Faraday cage' formed by C_{60} for an encapsulated N atom [6]. Notwithstanding the highly reactive nature of atomic nitrogen, electron paramagnetic resonance (EPR) spectroscopy shows that in $N@C_{60}$, nitrogen maintains its atomic ground state configuration—a striking and fascinating result [6].

It should be stressed that $N@C_{60}$ differs markedly from lanthanide endofullerenes in that there is negligible interaction or hybridisation of the atomic N states with the fullerene molecular orbitals. However, we have recently shown that the Ce atom in $Ce@C_{82}$ is also remarkably well-shielded from the chemical environment of the fullerene cage, despite the presence of a strong Ce–C_{82} interaction [7]. The motivation underlying our study of $Ce@C_{82}$ (detailed here and in other [7,27] papers) stems not only from an interest in electronic couplings and molecule-surface interactions in endofullerene systems, but from the intriguing physical properties of Ce itself. As discussed in detail by van der Eb [8], although the electronic configuration for *atomic* cerium is [Xe] $6s^24f^2$ pure Ce adopts a configuration between [Xe] $6s^25d^14f^1$ and [Xe] $6s^25d^24f^0$ in the bulk form, depending on the structural phase (notably, Ce is the only element with a solid–solid critical point). The ground state properties of Ce are generally described using one of two models where the 4f electrons are treated either in terms of a band formalism or as localized states which are weakly coupled to an itinerant conduction band [9,10]. In Ce compounds, the character of the 4f states and the overall electronic structure of the solid similarly depend strongly on 4f-conduction electron hybridisation. Given the distinct differences between the character of 4f electrons in cerium as compared to other lanthanides—in particular, their much less localized character—it is clear that $Ce@C_{82}$ represents an extremely important member of the endohedral fullerene family whose study has the potential to yield significant insights into the electronic behaviour of cerium.

Despite this intrinsic fundamental interest, $Ce@C_{82}$ remains one of the least studied endohedral fullerenes. Early work focused on the synthesis process and the valence of the Ce atom which, from an analysis of Ce 3d X-ray photoelectron spectra, was proposed to be 3+ [11,12]. Sato et al. [13] investigated the intramolecular dynamic motion of the Ce atom in the cage and found the presence of two different chemical species of $Ce@C_{82}$. X-ray diffraction (XRD) and Raman scattering measurements have also been utilized to characterize the structure of $Ce@C_{82}$ powders and thin films [14,15]. Here, we extend the study of $Ce@C_{82}$ to encompass scanning tunneling microscopy (STM) and photoelectron spectroscopy measurements of submonolayer coverages and thin films of the molecule on Ag:Si(1 1 1)-($\sqrt{3}\times\sqrt{3}$)R30° surfaces. (The reasons motivating our choice of this particular substrate are outlined in Section 2.) Although STM is a powerful tool to investigate the behaviour of endofullerenes on clean surfaces and has been successfully used to study, for example, submonolayer coverages of $La@C_{82}$ and $Y@C_{82}$ on metal and semiconductor substrates

[1] We realise that although the use of the terms "endohedral fullerene" and "$X@C_{82}$" have become widespread in the physics community, the correct IUPAC nomenclature is in fact "*incar*-fullerenes" and "*i*XC_{82}", denoting the incarceration of the atom within the molecular cage.

[16–18], no work on the adsorption/growth behaviour of Ce@C_{82} has been reported to date. Moreover, the electronic properties of Ce@C_{82} thin films and the interaction between the encapsulated Ce atom and the outer carbon cage have been investigated by synchrotron radiation photoemission spectroscopy (SR-PES) and X-ray photoelectron spectroscopy (XPS). Other publications by our group [7,27] describe resonant photoemission and NEXAFS spectroscopy of adsorbed Ce@C_{82} molecules where the effects of strong covalent adsorption (on silicon) on the electronic structure of the encapsulated atom are of primary interest. Here, our focus is on the electronic structure of submonolayers and thin films of Ce@C_{82} on a substrate (Ag:Si(1 1 1)-($\sqrt{3}\times\sqrt{3}$)R30°) with which the fullerene molecules interact extremely weakly.

2. Experimental

Clean Si(1 1 1)-(7×7) surfaces were obtained by degassing samples at ~600 °C for 8–12 h and then flash annealing at ~1200 °C for 15–30 s with direct current sample heating (under ultrahigh vacuum (UHV) conditions). The Ag:Si(1 1 1)-($\sqrt{3}\times\sqrt{3}$)R30° (henceforth, Ag:Si-$\sqrt{3}$) surfaces were prepared by depositing Ag onto the clean Si (1 1 1)-(7×7) surface while the substrate was kept at ~500 °C. During each of these processes, the UHV chamber pressure was below 1×10^{-9} Torr. The Ce@C_{82} material was produced and purified as described elsewhere [19], and stored in CS_2. Before deposition onto the clean Ag-terminated Si(1 1 1) surface, the endohedral fullerene material was degassed at 200 °C for 24 h in a custom-built evaporator comprising a Knudsen cell mounted on a linear transfer arm. (The evaporator could be isolated from the main chamber via a gate valve.) Ce@C_{82} was then sublimed onto the Ag-terminated Si(1 1 1) surface (which was held at room temperature) by rapidly (~10 min) increasing the endohedral fullerene source temperature to ~600 °C.

It is important to stress that the distance between the crucible containing the endohedral fullerene material and the sample surface was reduced to ~1 cm by use of the linear transfer arm. We find—in common with other groups [20]—that a short sample–source distance (and a relatively rapid temperature rise) is essential in order to fabricate a thick endofullerene film. Due to the rapid increase in source temperature, during the endofullerene deposition the chamber pressure rose to a maximum value of 2×10^{-8} Torr (and fell steadily during the 20 min deposition period).

The high chamber pressure during endofullerene deposition necessitates the use of a substrate which is rather more chemically inert than the Si(1 1 1)-(7×7) reconstruction—this is one reason why the Ag:Si(1 1 1)-($\sqrt{3}\times\sqrt{3}$)R30° ('Ag-passivated') surface is chosen as the initial substrate. (A second reason relates to the relatively large diffusion coefficients of (endo)fullerene molecules on Ag:Si-(1 1 1), permitting the formation of large, well-ordered molecular islands and monolayers.) In control experiments we found that the uptake of contaminants on the Ag:Si(1 1 1) surface following exposure to total chamber pressures of order 10^{-8} Torr was negligible. Similarly, following deposition of the Ce@C_{82} film, photoemission measurements verified the absence of oxygen and CS_2 contamination. The fabrication of C_{82} films followed a similar method to that used for the preparation of the Ce@C_{82} films: namely, degassing at 200 °C for 24 h with subsequent deposition at ~600 °C.

Room temperature STM observations were performed in a UHV STM system with a base pressure of $\sim1\times10^{-10}$ Torr using electrochemically etched W tips. Although the UHV microscope is from a commercial source (WA Technology), the control electronics and software have been developed in-house [21]. For the STM measurements a substantially lower endofullerene deposition rate was employed (0.001–0.01 ML/h) to deposit submonolayer coverages. This rate was determined simply by counting the number of Ce@C_{82} molecules in a given scan area and averaging over a number of images taken at different regions of the surface. Photoemission measurements of Ce@C_{82} films were carried out on beamline 5U1 of the synchrotron radiation source (SRS), Daresbury, UK using a single channel hemispherical analyser and a total instrumental resolution (as

estimated from the Fermi edge broadening of the Ta sample holder) of ~150 meV. The photoemission measurements on C_{82} films were taken on beamline I311 of MAXII, Sweden using a UHV chamber equipped with a hemispherical electron energy analyser (SCIENTA SES200) but with substantially better energy resolution (<50 meV). All valence band measurements were taken at room temperature and at normal emission with the angle between the incident beam and the analyser fixed at 45° (Daresbury) or 55° (MAXII). The Ce 3d core level spectrum of the sample exposed to atmosphere was measured by a Kratos AXIS Ultra X-ray photoelectron spectrometer with monochromatized Al K_α radiation (1468.6 eV) operated at 10 mA emission current and 15 kV anode potential. Ce 3d spectra were also acquired on beamline ID32 of the ESRF using a hemispherical analyser positioned at 45° to the incoming beam and with a photon energy resolution of ~260 meV (at a photon energy of 2610 eV).

3. Results and discussion

3.1. Adsorption of Ce@C_{82} molecules on the Ag/Si(111)-($\sqrt{3}\times\sqrt{3}$)R30° surface: submonolayer coverages

Fig. 1 shows STM images of different coverages of Ce@C_{82} on the Ag:Si-$\sqrt{3}$ surface. In Fig. 1(a), a typical STM image of a low endofullerene coverage (0.005 ML), the bright circular features are the absorbed Ce@C_{82} molecules. No evidence for electric dipole-driven formation of isolated endofullerene units such as dimers or the triangular clusters previously observed for Nd@C_{82} on C_{60} films [22], has been found at any time during our STM measurements. It should be borne in mind, however, that while the (endo)fullerene–Ag:Si-$\sqrt{3}$ interaction is weak and largely van der Waals in character [23–25], electrical measurements have suggested that a small amount of charge transfer may be involved [24]. The degree to which this type of charge transfer might influence the bonding of Ce@C_{82} to the Ag:Si-$\sqrt{3}$ surface is as yet unknown and will be the focus of a future study by our group.

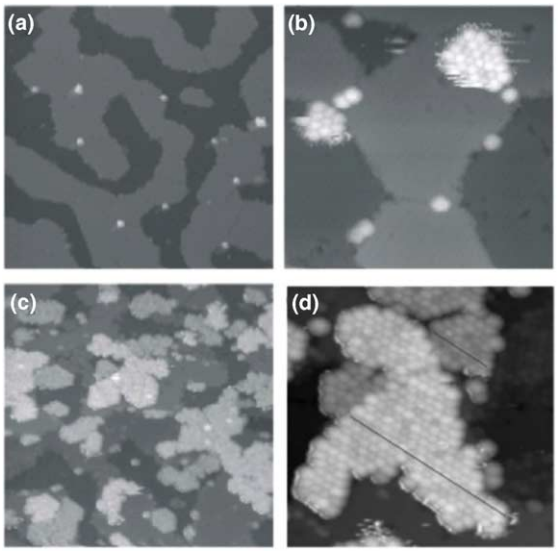

Fig. 1. STM images of different coverages of Ce@C_{82} on the Ag:Si-$\sqrt{3}$ surface. (a) 0.005 ML, −3 V, 0.1 nA, 90×90 nm; (b) 0.1 ML, −2 V, 0.1 nA, 32×32 nm; (c) 0.4 ML, −3 V, 0.1 nA, 86×86 nm; (d) A high resolution image of a 0.4 ML coverage where the orientation of individual molecular domains may be discerned. (Lines on the image highlight orientation of domains and are drawn as a guide to the eye.)

The molecules observed in Fig. 1(a) are isolated and bound at step edges, defects and domain boundaries of the Ag:Si-$\sqrt{3}$ reconstruction, i.e. reactive sites which are associated with Si dangling bonds. Further deposition of Ce@C_{82} leads to the formation of small islands (Fig. 1(b)). The islands are close packed and again grown from the reactive sites on the surface. Moreover, in a small number of cases domains with different orientations are observed (Fig. 1(b)). The angle between the primary vectors of the two islands shown in Fig. 1b is 30° ± 2°. For La@C_{82} on Ag:Si-$\sqrt{3}$, only one domain identified as having (3×3) order is observed for coverages up to 0.5 ML [16]. This (3×3) phase was also by far the most common of those observed at a coverage of 0.7 ML [16], accounting for 86% of the La@C_{82}-covered surface area. Unfortunately, due to poor experimental resolution we could not successfully resolve both the Ag:Si-$\sqrt{3}$ reconstruction and the Ce@C_{82} islands simultaneously. It is thus not possible to determine the orientation of the islands with respect to the substrate in-plane crystallographic axes.

Nevertheless, given the molecular separation within the domains (1.16 nm) and the ~30° angle between the basis vectors of the islands, the domains we observe most likely correspond to the (3×3) and ($7\sqrt{3}\times7\sqrt{3}$)R30° phases observed for La@C_{82} on Ag:Si-$\sqrt{3}$ (see Table 1 of Ref. [16]).

Larger islands are formed with increasing coverage (Fig. 1(c)). It is worth noting that all of the islands have the same orientation, as shown in Fig. 1(d). This contrasts with the variety of domains observed for La@C_{82} on Ag:Si-$\sqrt{3}$ [16]. Although it might perhaps be tempting to associate these differences in molecular ordering with variations in intermolecular and molecule–substrate interactions for Ce@C_{82} as compared to La@C_{82}, note that the deposition rate used in the present study differs rather dramatically from that used in Ref. [16] (0.001–0.01 ML/h (this work) as compared to 0.1 ML/h [16]). Hence, it is most likely that growth kinetics can largely account for the slight differences in overall molecular packing observed for Ce and La endofullerenes on Ag:Si-$\sqrt{3}$. (In this context, it is also worth noting that following annealing at 300 °C, only one La@C_{82} domain remained on the Ag:Si-$\sqrt{3}$ surface [16].)

3.2. Growth of Ce@C_{82} thin films

Fig. 2 shows STM images of a thick Ce@C_{82} film on the Ag/Si(1 1 1) surface. From Fig. 2(a), a large area STM image, more than 10 layers can be clearly distinguished. Close examination of the surface of the film, as shown in Fig. 2(b), shows that the layers all have the same orientation. As also shown in the high resolution image in Fig. 2(c), the endofullerene thin film is highly ordered. From an STM profile measurement, the separation of the molecules is measured as 1.12 ± 0.02 nm. X-ray diffraction (XRD) measurements of a mixture of two Ce@C_{82} isomers [14] and a sublimed Ce@C_{82} sample [15] reveal that the crystal structure of the samples in each case is face-centred cubic (fcc) with lattice constants of 1.588 and 1.577 nm respectively. The results of a C 1s near-edge X-ray absorption fine spectrum (NEXAFS) study of Ce@C_{82} [7] are also consistent with the 4:1 isomeric mix very recently reported by Shi-

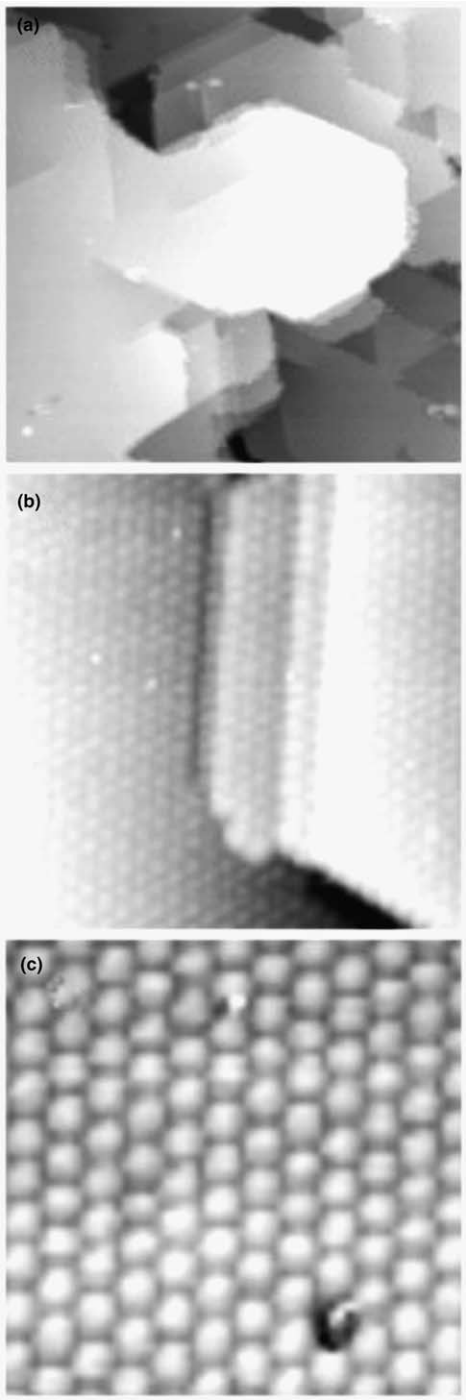

Fig. 2. STM images of a Ce@C_{82} thin film grown on Ag:Si-$\sqrt{3}$. (a) 158×158 nm, −3 V, 0.1 nA; (b) 26×26 nm, −3 V, 0.1 nA; (c) 12×12 nm, −3 V, 0.1 nA, the inset −3 V, 0.1 nA, 30 nm×30 nm.

bata et al. [14]. Assuming that the crystal structure of the film is fcc, and using the distance between the molecules on fcc(1 1 1) planes obtained from STM images similar to that shown in Fig. 2(c), the lattice constant is 1.58 ± 0.03 nm, which is in excellent agreement with the previous XRD results [14,15].

3.3. Electronic structure of $Ce@C_{82}$ thin films

Fig. 3 shows valence band spectra ($h\nu = 60$ eV) of both a $Ce@C_{82}$ film and a C_{82} film on the Ag:Si-$\sqrt{3}$ surface. (Note that attempting to isolate the Ce-derived density of states via a $Ce@C_{82}$–C_{82} difference spectrum is both problematic and misleading. This is because structural (isomeric) differences between the C_{82} and $Ce@C_{82}$ samples strongly affect the valence band spectra.) No Ag or Si core-level signals were detected, indicating that the contribution of the substrate can be safely ignored. Although the overall spectral 'signature' of $Ce@C_{82}$ is rather similar to that of C_{82}, there are significant differences in the low binding energy features (within a few volts of the Fermi level). The spectral onset of C_{82} is much deeper (>1 eV) due to the higher ionization energy of the empty fullerene.

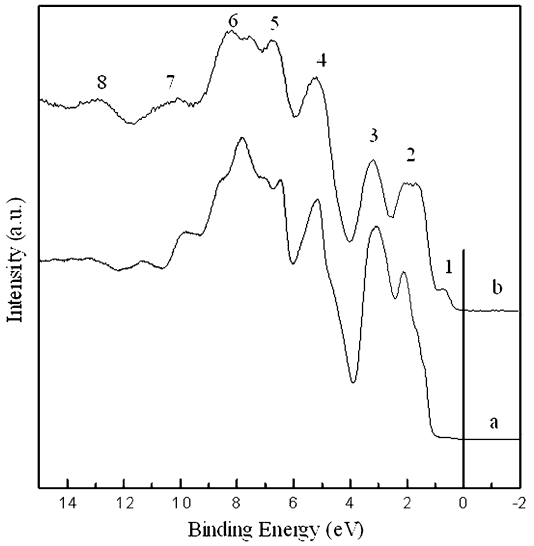

Fig. 3. Comparison of the valence band spectra of the $Ce@C_{82}$ ordered film and C_{82} film. The incident photon energy is 60 eV. (a) C_{82} film; (b) $Ce@C_{82}$ film.

Furthermore, the peak labelled '1' in Fig. 3(b) is completely absent from Fig. 3(a) and the overall shape of the band centred at ~1.65 eV for $Ce@C_{82}$ (peak 2) is also quite different from its counterpart in C_{82}. It is also important to note that there are isomeric differences between the C_{82} and $Ce@C_{82}$ samples used in our study.

The valence band of the $Ce@C_{82}$ film is markedly similar to that of both $La@C_{82}$ [4] and $Gd@C_{82}$ [26], i.e. metallofullerenes with a trivalent (or close to trivalent) encapsulated atom. In particular, in common with Poirier et al. [4], we can identify eight features (those labelled 1–8 in Fig. 3(b)) in the endofullerene valence band spectrum. Peak 1, located at 0.73 eV below the Fermi level, has a direct counterpart in the valence band spectra of $La@C_{82}$ [4] and $Gd@C_{82}$ [26] which (along with the next highest binding energy valence band feature) has been identified as arising from charge transfer from the encapsulated atom to the fullerene cage. While Poirier et al. originally suggested that this so-called 'single occupied molecular orbital (SOMO)' feature was 'almost entirely' C derived and associated with minimal La 5d character, a comprehensive resonant photoemission study by Kessler et al. [5] clearly highlighted that the frontier valence orbitals contain significant La character. Similarly, attempts to quantify the amount of charge transferred from the encapsulated atom on the basis of the integrated intensities of near-Fermi level valence band features [26], are somewhat flawed due to the strong final state photoelectron interference effects observed in fullerene systems. Hence, although valence band measurements (Fig. 3), Ce 3d XPS spectra (Fig. 4 and Ref. [11]), and Ce $L_{4,5}$ NEXAFS [7] data are consistent with a Ce charge state that is close to 3+, we have recently bolstered these spectroscopic techniques with comprehensive Ce $3d \rightarrow 4f$ and Ce $4d \rightarrow 4f$ RESPES studies of both $Ce@C_{82}$ and $Ce_2@C_{80}$ to elucidate the degree of Ce 4f occupancy in each case [27].

Despite the partly filled molecular orbitals resulting from $Ce \rightarrow C\text{-}\pi^*$ charge transfer, there is clearly no evidence of density of states at the Fermi level in Fig. 3(b). The spectral onset of the valence band spectrum of the ordered $Ce@C_{82}$ film is located at 0.3 eV below the Fermi level, suggesting

that Ce@C_{82} film is semiconducting and its band gap is at least 0.3 eV. (The transport gap is defined by the separation of the HOMO measured in an 'electron subtraction' technique such as photoemission and the LUMO measured in an 'electron addition' spectroscopy such as inverse photoemission.) In good agreement with the results of our valence band study, Shibata et al. recently measured the temperature dependence of the resistance of a Ce@C_{82} thin film and estimated the band gap as 0.4 eV [14].

3.4. Interaction between the encapsulated Ce atom and the fullerene cage

Fig. 4 shows the Ce 3d core level spectra of the Ce@C_{82} film before and after exposure to atmosphere for more than 10 months. Both spectra comprise $3d_{3/2}$–$3d_{5/2}$ spin-orbit-split doublets with

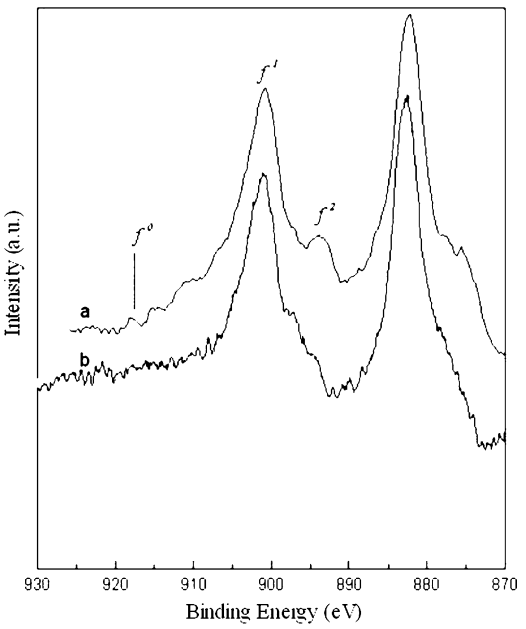

Fig. 4. Ce 3d core level spectra of a Ce@C_{82} film before and after atmospheric exposure for a period of approximately 10 months. (a) Spectrum for the as-prepared sample, the incident photon energy is 2610 eV (taken on beamline ID32, ESRF); (b) Spectrum for the sample exposed to air, the incident photon energy is 1468.6 eV (acquired using a Kratos AXIS Ultra X-ray photoelectron spectrometer with monochromatized Al K_α radiation (1468.6 eV)).

substantial final-state related satellite structure. In the early eighties, Gunnarson and Schönhammer developed an Anderson impurity-related theoretical model to calculate XPS, XAS, and valence photoemission spectra for Ce compounds [28]. Their analysis, coupled with a series of subsequent experimental studies, has shown that Ce 3d spectra may generally be interpreted in terms of a superposition of three different final states: $3d^94f^0$, $3d^94f^1$ and $3d^94f^2$. The binding energy positions and spectral features associated with each of these states are labelled f^0, f^1, and f^2 for the $3d_{3/2}$ component in Fig. 4. The intensity of the f^0 feature is proportional to $1-n_f$, where n_f is the 4f electron count in the initial state [29]. That a distinct peak related to the $4f^0$ state (binding energy ~ 914 eV) is not observed in Fig. 4 reveals that the 4f occupancy in the initial state is close to 1, i.e. the Ce valence is close to 3+. A similar observation was made by Ding et al. [8]. It is important to stress, however, that—as pointed out by both Fuggle et al. [29] and Ohno [30]—while the intensity of the $3d^94f^0$ peak 'tracks' the value of the 4f occupancy, the agreement is not exact. RESPES represents a somewhat more reliable method of detecting Ce 4f occupancy and we will present the results of our Ce@C_{82} RESPES measurements in a separate paper [27].

A comparison of the Ce 3d spectra for as-deposited and air-exposed Ce@C_{82} films (see Fig. 4(a) and (b)) clearly illustrates that there are only subtle spectral differences following exposure of the endofullerene film to atmosphere for over 10 months. The continued absence of a $3d^94f^0$-related peak in the Ce 3d spectrum indicates that there is certainly little or no cerium(IV) oxide (in the form of CeO_2) present following the exposure to atmosphere [31]. Furthermore, the overall Ce 3d lineshape is very different from that expected for Ce(III) oxide [32]. Although the minor changes we observe in the Ce 3d spectrum following atmospheric exposure of the Ce@C_{82} film (largely in the 890–900 eV binding energy region) may relate to small modifications in the cerium oxidation state, it should be borne in mind that the spectrum shown in Fig. 4(a) was acquired at a rather different photon energy that that shown in Fig. 4(b) (1468.6 and 2610 eV respectively). Thus, we cannot at present rule out the possibility that variations in

photoabsorption cross section are responsible for the differences we observe. In any case, however, our Ce 3d data clearly highlight the high degree of protection offered by the C_{82} cage to the encapsulated cerium atom. This observation echoes that of a recent study of the interaction of $Ce@C_{82}$ with the Si(1 1 1) surface where, despite the formation of exceptionally strong covalent bonds between the fullerene cage and the silicon substrate, the Ce electronic structure and valence—as probed by Ce $L_{4,5}$ NEXAFS—remained remarkably impervious to dramatic changes in the molecular chemical environment [7].

4. Conclusions

We have studied the adsorption behaviour and thin film growth of $Ce@C_{82}$ molecules on Ag-terminated Si(1 1 1) surfaces. The molecules preferentially adsorb at the reactive sites, such as defects, step edges and domain boundaries of the Ag:Si-$\sqrt{3}$ reconstruction due to the weak interaction between $Ce@C_{82}$ and the Ag-passivated surface. At relatively low coverages ($\sim$0.4 ML), the molecular islands each have the same orientation with an intermolecular separation of 1.16 nm. Very well-ordered fcc thin films of $Ce@C_{82}$ with few defects may be grown on the Ag:Si-$\sqrt{3}$ surface. Valence band spectroscopy reveals that the $Ce@C_{82}$ film is semiconducting with a band gap of at least 0.3 eV. Our valence band and Ce 3d XPS data, taken together, strongly suggest that the Ce valence is close to 3+. The fullerene cage strongly isolates the encapsulated Ce atom from the chemical surroundings and largely maintains the electronic state of Ce atom following prolonged exposure of a $Ce@C_{82}$ film to atmosphere.

Acknowledgments

T.J.S.D. thanks the Royal Society for a Joint Research Project—Japan. We acknowledge funding by the UK Engineering and Physical Sciences Research Council (EPSRC) under grant GR/1880/01 and by the European Large Scale Facilities Programme for provision of funding for the experiments at MaxLAB. We also acknowledge MaxLAB for provision of synchrotron radiation on beamline I3-11, the ESRF for provision of beamtime on BL ID32, and the UK Council for the Central Laboratory of the Research Councils (CCLRC) for the provision of beamtime at Daresbury SRS. The beamtime experiments were facilitated by the expert technical assistance of George Miller, whom we sincerely thank.

References

[1] J.R. Health, S.C. O'Brien, A. Zhang, Y. Liu, R.F. Curl, H.W. Kroto, F.K. Tittel, R.E. Samlley, J. Am. Chem. Soc. 107 (1985) 7779.
[2] R.D. Beck, P. Weis, J. Rockenberger, M.N. Kappas, Surf. Sci. Lett. 3 (1996) 771;
M. Takata, B. Umibeda, E. Nishibori, M. Sakata, Y. Saito, M. Ohno, H. Shinohara, Nature 377 (1995) 46.
[3] H. Shinohara, Rep. Prog. Phys. 63 (2000) 843.
[4] M.D. Poirier, M. Knupfer, J.H. Weaver, W. Andreoni, K. Laasonen, M. Parrinello, D.S. Bethune, K. Kikuchi, Y. Achiba, Phys. Rev. B 49 (1994) 17403.
[5] B. Kessler, A. Bringer, S. Gramm, C. Schlebusch, W. Eberhardt, Phys. Rev. Lett. 79 (1997) 2289.
[6] T. Murphy, T. Pawlik, A. Weidinger, M. Hohne, R. Alcala, J.M. Spaeth, Phys. Rev. Lett. 77 (1996) 1075.
[7] K. Schulte, L. Wang, P. Moriarty, J.A. Purton, S. Patel, H. Shinohara, M. Kanai, T.J.S. Dennis, Phys. Rev. B, submitted.
[8] 'Cerium, one of Nature's purest puzzles', Jeroen van der Eb, PhD Thesis, Rijksuniversitet Groningen (2000).
[9] D. Glötzel, J. Phys. F 8 (1978) L163.
[10] P. Coleman, Phys. Rev. B 29 (1984) 3035.
[11] J. Ding, L. Weng, S. Yang, J. Phys. Chem. 100 (1996) 11120.
[12] B. Liu, G. Zou, H. Yang, S. Yu, J. Lu, Z. Liu, S. Liu, W. Xu, J. Phys. Chem. Solids 11 (1997) 1873.
[13] W. Sato, K. Sucki, K. Kikuchi, K. Kobayashi, S. Suzuki, Y. Achiba, H. Nakahara, Y. Ohkubo, F. Ambe, K. Asai, Phys. Rev. Lett. 80 (1998) 133.
[14] K. Shibata, Y. Rikishi, T. Hosokawa, Y. Haruyama, Y. Kubozono, S. Kashino, T. Uruga, A. Fujiwara, H. Kitagawa, T. Takano et al., Phys. Rev. B 68 (2003) 094104.
[15] C. Nuttall, Y. Inada, Y. Watanabe, K. Nagai, T. Nuro, D. Chi, T. Takenobu, Y. Iwasa, K. Kikuchi, Mol. Cryst. Liq. Cryst. 340 (2000) 635.
[16] M.J. Butcher, J.W. Nolan, M.R.C. Hunt, P.H. Beton, L. Dunsch, P. Kuran, P. Gorgi, T.J.S. Dennis, Phys. Rev. B 64 (2001) 195401.
[17] Y. Hasegawa, Y. Ling, S. Yamazaki, T. Hahsizume, H. Shinohara, A. Sakai, H.W. Pickering, T. Sakurai, Phys. Rev. B 56 (1997) 6470.
[18] C. Ton-That, A.G. Shard, S. Egger, A. Taninaka, H. Shinohara, M.E. Welland, Surf. Sci. Lett. 522 (2003) L15.

[19] M. Kanai, T.J.S. Dennis, H. Shinohara, AIP Conf. Proc. 633 (2002) 35.
[20] Cuong Ton-That, private communication (2002).
[21] M.J. Humphy, R. Chettle, P. Moriarty, M.D. Upward, P.H. Beton, Rev. Sci. Inst. 71 (2000) 1698.
[22] N. Lin, H. Huang, S. Yang, N. Cue, Phys. Rev. B 58 (1998) 2126.
[23] M.J. Butcher, Adsorption and Manipulation of Doped Fullerenes on Silicon Surfaces, PhD Thesis, University of Nottingham (2000).
[24] S. Hasegawa, K. Tsuchie, K. Toriyma, X. Tong, T. Nagao, Appl. Surf. Sci. 162 (2000) 42.
[25] M.D. Upward, P. Moriarty, P.H. Beton, Phys. Rev. B 56 (1997) R1704.
[26] S. Hino, K. Umishita, K. Iwasaki, T. Miyazaki, T. Miyamae, K. Kikuchi, Y. Achiba, Chem. Phys. Lett. 281 (1997) 115.
[27] K. Schulte, L. Wang, M. Kanai, T.J.S. Dennis, J. Anderson, S. Gorovikov, J. Purton, S. Patel, P. Moriarty (unpublished).
[28] O. Gunnarsson, K. Schönhammer, Phys. Rev. B 28 (1983) 4315.
[29] J.C. Fuggle, et al., Phys. Rev. B 27 (1983) 4637.
[30] Y. Ohno, Phys. Rev. B 48 (1993) 5515.
[31] J.P. Holgado, R. Alvarez, G. Munnuera, Appl. Surf. Sci. 161 (2000) 301.
[32] D.R. Mullins, S.H. Overbury, D.R. Huntley, Surf. Sci. 409 (1998) 307.